Spectrochimica Acta Part A: Molecular and Biomolecular Spectroscopy 153 (2016) 257–267

Contents lists available at ScienceDirect

Spectrochimica Acta Part A: Molecular and Biomolecular Spectroscopy

journal homepage: www.elsevier.com/locate/saa

# Highly efficient simultaneous ultrasonic assisted adsorption of brilliant green and eosin B onto ZnS nanoparticles loaded activated carbon: Artificial neural network modeling and central composite design optimization

M. Jamshidi [a], M. Ghaedi [a,*], K. Dashtian [a], A.M. Ghaedi [b], S. Hajati [c], A. Goudarzi [d], E. Alipanahpour [a]

[a] Chemistry Department, Yasouj University, Yasouj 75918-74831, Iran
[b] Science, Gachsaran Branch, Islamic Azad University, P.O. Box 75818-63876, Gachsaran, Iran
[c] Physics Department, Yasouj University, Yasouj 75914-35, Iran
[d] Department of Polymer Engineering, Golestan University, Gorgan 49188-88369, Iran

ARTICLE INFO

*Article history:*
Received 19 May 2015
Received in revised form 5 August 2015
Accepted 11 August 2015
Available online 17 August 2015

*Keywords:*
Brilliant green
Eosin B
Response surface methodology
Artificial neural network
Simultaneous removal

ABSTRACT

In this work, central composite design (CCD) combined with response surface methodology (RSM) and desirability function approach (DFA) gives useful information about operational condition and also to obtain useful information about interaction and main effect of variables concerned to simultaneous ultrasound-assisted removal of brilliant green (BG) and eosin B (EB) by zinc sulfide nanoparticles loaded on activated carbon (ZnS-NPs-AC). Spectra overlap between BG and EB dyes was extensively reduced and/or omitted by derivative spectrophotometric method, while multi-layer artificial neural network (ML-ANN) model learned with Levenberg–Marquardt (LM) algorithm was used for building up a predictive model and prediction of the BG and EB removal. The ANN efficiently was able to forecast the simultaneous BG and EB removal that was confirmed by reasonable numerical value i.e. MSE of 0.0021 and $R^2$ of 0.9589 and MSE of 0.0022 and $R^2$ of 0.9455 for testing data set, respectively. The results reveal acceptable agreement among experimental data and ANN predicted results. Langmuir as the best model for fitting experimental data relevant to BG and EB removal indicates high, economic and profitable adsorption capacity (258.7 and 222.2 mg $g^{-1}$) that supports and confirms its applicability for wastewater treatment.



## 1. Introduction

Wide application of dyes in versatile industries and/or medicinal or food activities increases [1–3] problems such as toxicity, carcinogenicity, mutagenic, teratogenic problems, and hazards for some microorganisms [4,5]. These contaminants have adverse effects on human health that stress to the researchers' for their removal to achieve safe and clean media [6,7]. Dyes enter to organism life via pulmonary and digestive system (water or food) [8,9] that cause requirement of preliminary clean up procedure before their entrance to water bodies. Coagulation, adsorption, membrane filtration, electrochemical techniques, and biosorption facilitated pollutants content reduction to values lower than threshold limit [10,11]. Adsorption due to higher efficiency, lower cost, and simplicity [1,4,12], especially based on safe and green nanostructure materials is a popular method to achieve high removal percentage and higher adsorption capacity in a short time. This requirement is simply met by application of novel nanomaterial loaded on conventional supports like activated carbon. Their very lower size and high surface structure in compromise to great number of activated carbon functional groups and porous structure permit to obtain fast adsorption kinetics in very polluted media [13–15].

Ultrasound because of the acoustic cavitations phenomenon (growth and collapse of tiny bubbles) due to pressure wave propagation through liquid accelerates and improves mass transfer [14,15].

The experimental design method known as design of experiment (DOE) is a powerful and economic tool for simultaneous optimization purposes to provide better estimation of the importance of each input parameter and their interactions [16,17]. Moreover, the behavior of each system as function of effective factors can be predicted through DOE [14] following assessment of global optimal conditions which are based on Derringer's desirability function [18,19]. Modeling the adsorption process has been undertaken by various methods including multiple linear regression (MLR), partial least squares (PLS), principal component regression (PCR), support vector regression (SVR), adaptive network-based fuzzy inference system (ANFIS), and artificial neural networks (ANNs). Among these methods, the ANN extensively was used for modeling complex nonlinear systems and solving problems in various areas [3,8,20–24].

In this work, central composite design (CCD) that was used for optimization of variables (sonication time, initial dyes concentration and amount of adsorbent) corresponds to simultaneous ultrasonic

* Corresponding author.
*E-mail address:* m_ghaedi@mail.yu.ac.ir (M. Ghaedi).

http://dx.doi.org/10.1016/j.saa.2015.08.024
1386-1425/

assisted removal of brilliant green (BG) and eosin B (EB) (Fig. 1a, b). Spectra overlap between BG and EB spectrum was resolved by derivative spectrophotometric method. The importance of model, main, and interaction of factors was approximately estimated by analysis of variance (ANOVA). The runs that correspond to CCD were inputs for three-layer ANN model by a back propagation (BP) algorithm to predict the efficiency of ZnS-NP-AC for BG and EB adsorption. Then, isotherm models suitable for fitting experimental data that correspond to BG and EB removal were found to be Langmuir model.

## 2. Experimental

### 2.1. Materials and apparatus

All chemicals without further purification were supplied from Merck, Dermasdat, Germany. Zinc acetate dihydrate ($Zn(CH_3COO)_2$, $2H_2O$), acid acetic ($CH_3COOH$) and thioacetamide ($CH_3CSNH_2$) was purchased from Sigma-Aldrich company. Here, zinc acetate and thioacetamide were used as the source of $Zn^{2+}$ and $S^{2-}$ ions, respectively. Acid acetic was implied as a complexing agent for $Zn^{2+}$ ions and activated carbon was used as a support material for loading ZnS-NPs. Ammonia solution ($NH_4OH$) was used as a hydroxide source as well as a complexing agent for $Zn^{2+}$ ions and provided by Chem lab Company. The morphology of the nanoparticles was observed by field emission scanning electron microscopy (FE-SEM: Hitachi S-4160) operating under an acceleration voltage of 15 KV. A Fourier transform infrared (FT-IR) spectrum was recorded using a Perkin Elmer-Spectrum RX-IFTIR spectrometer in the range of 400–4000 $cm^{-1}$. X-ray diffraction (XRD, Philips PW 1800) was performed to characterize the phase and structure of the prepared nanoparticles using Cukα radiation (40 KV and 40 mA) at angles ranging from 10 to 80°. An ultrasonic bath with heating system (Tecno-GAZ SPA Ultra Sonic System) at 40 kHz of frequency and 130 W of power was

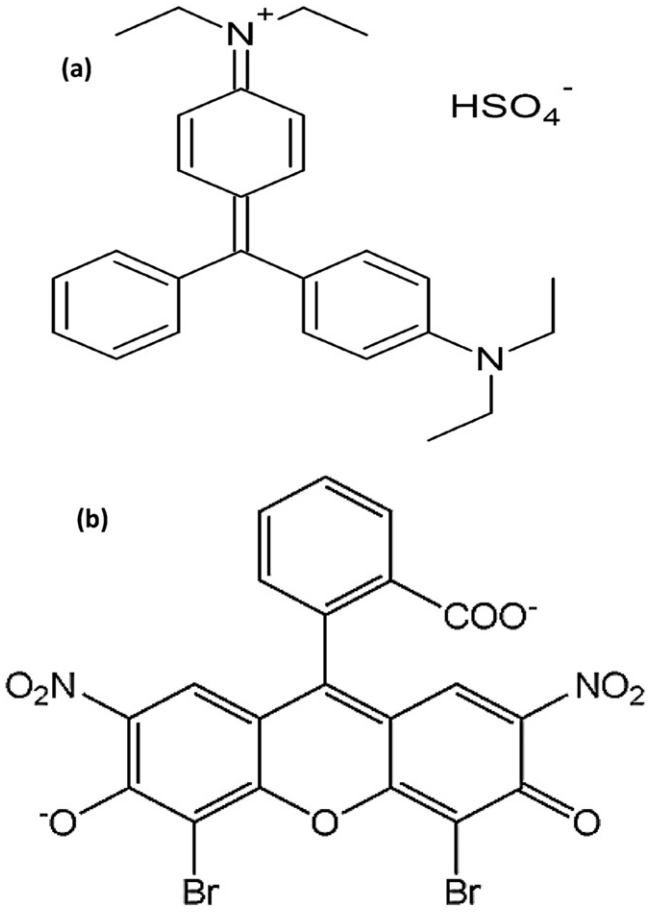


**Fig. 1.** Chemical structure of brilliant green (a) and eosin B (b) at different mg $L^{-1}$ BG.

**Table 1**
Experimental factors and levels in the central composite design.

| Factors | Unit | Surface factors | | | | |
|---|---|---|---|---|---|---|
| | | Levels | | | Star point α = 2 | |
| | | (Low) −1 | (Central) 0 | (High) +1 | −α | +α |
| (X1) contact time | Min | 3 | 4 | 5 | 2 | 6 |
| (X2) adsorbent dosage | mg | 15 | 20 | 25 | 10 | 30 |
| (X3) BG concentration | mg $L^{-1}$ | 4.5 | 7 | 9.5 | 2 | 12 |
| (X4) EB concentration | mg $L^{-1}$ | 6.5 | 9 | 11.5 | 4 | 14 |

**Table 2**
Experimental conditions and values obtained through the CCD.

| Runs | Block | $X_1$ | $X_2$ | $X_3$ | $X_4$ | BG removal (%) | EB removal (%) |
|---|---|---|---|---|---|---|---|
| 1 | 1 | 4 | 10 | 7 | 9 | 66.7 | 65 |
| 2 | 1 | 5 | 25 | 9.5 | 11.5 | 96.1 | 95.3 |
| 3 | 1 | 4 | 20 | 7 | 9 | 95.4 | 94 |
| 4 | 1 | 3 | 15 | 9.5 | 11.5 | 78 | 81.4 |
| 5 | 1 | 4 | 20 | 7 | 14 | 94.9 | 87.9 |
| 6 | 1 | 5 | 15 | 4.5 | 6.5 | 89.1 | 90 |
| 7 | 1 | 5 | 15 | 4.5 | 11.5 | 90.1 | 84 |
| 8 | 1 | 4 | 20 | 7 | 9 | 96 | 95.1 |
| 9 | 1 | 2 | 20 | 7 | 9 | 91.7 | 89.4 |
| 10 | 1 | 3 | 25 | 9.5 | 6.5 | 93.2 | 97.3 |
| 11 | 1 | 3 | 15 | 4.5 | 11.5 | 81.5 | 80 |
| 12 | 1 | 5 | 25 | 4.5 | 6.5 | 99.9 | 99.8 |
| 13 | 1 | 3 | 15 | 4.5 | 6.5 | 83.4 | 83.2 |
| 14 | 1 | 4 | 20 | 7 | 9 | 95.5 | 94 |
| 15 | 1 | 4 | 20 | 7 | 9 | 96.4 | 94.3 |
| 16 | 1 | 4 | 20 | 7 | 9 | 96.5 | 94.5 |
| 17 | 2 | 5 | 25 | 9.5 | 6.5 | 98.1 | 99.9 |
| 18 | 2 | 4 | 20 | 2 | 9 | 98.8 | 96.1 |
| 19 | 2 | 6 | 20 | 7 | 9 | 96.7 | 95.7 |
| 20 | 2 | 3 | 25 | 9.5 | 11.5 | 95.6 | 95.4 |
| 21 | 2 | 3 | 15 | 9.5 | 6.5 | 81 | 79 |
| 22 | 2 | 3 | 25 | 4.5 | 6.5 | 99.7 | 99.6 |
| 23 | 2 | 5 | 15 | 9.5 | 6.5 | 85.1 | 90.2 |
| 24 | 2 | 4 | 20 | 7 | 9 | 96.8 | 91.5 |
| 25 | 2 | 5 | 15 | 9.5 | 11.5 | 85.3 | 84.7 |
| 26 | 2 | 4 | 20 | 12 | 9 | 88.9 | 92.1 |
| 27 | 2 | 4 | 20 | 7 | 9 | 94 | 94.4 |
| 28 | 2 | 5 | 25 | 4.5 | 11.5 | 99.9 | 96.3 |
| 29 | 2 | 4 | 30 | 7 | 9 | 100 | 98.4 |
| 30 | 2 | 3 | 25 | 4.5 | 11.5 | 99.4 | 94 |
| 31 | 2 | 4 | 20 | 7 | 4 | 96.1 | 98.9 |
| 32 | 2 | 2.5 | 18 | 11 | 13 | 81.11 | 84.89 |
| 33 | 2 | 2.5 | 22 | 8 | 5 | 94.2 | 94.5 |
| 34 | 2 | 4.5 | 18 | 11 | 13 | 87.4 | 88.6 |
| 35 | 2 | 4.5 | 28 | 8 | 5 | 97.2 | 100 |
| 36 | 2 | 3.5 | 18 | 11 | 13 | 84.8 | 87.1 |
| 37 | 2 | 3.5 | 22 | 8 | 5 | 96.3 | 97.7 |
| 38 | 2 | 3.5 | 28 | 8 | 13 | 97.7 | 94.2 |
| 39 | 2 | 4.5 | 28 | 8 | 13 | 97.7 | 93 |
| 40 | 2 | 4.5 | 22 | 11 | 5 | 93.6 | 98.8 |
| 41 | 3 | 2.5 | 28 | 8 | 13 | 96.6 | 94.9 |
| 42 | 3 | 2.5 | 18 | 11 | 5 | 83.2 | 85.1 |
| 43 | 3 | 3.5 | 28 | 8 | 5 | 97.6 | 100 |
| 44 | 3 | 3.5 | 22 | 11 | 13 | 91.3 | 93 |
| 45 | 3 | 4.5 | 28 | 11 | 5 | 93.3 | 99.8 |
| 46 | 3 | 4.5 | 18 | 8 | 13 | 91.4 | 87.8 |
| 47 | 3 | 2.5 | 28 | 8 | 5 | 96.9 | 98.5 |
| 48 | 3 | 2.5 | 22 | 11 | 13 | 88.6 | 91.9 |
| 49 | 3 | 3.5 | 22 | 8 | 13 | 95.6 | 92.6 |
| 50 | 3 | 3.5 | 18 | 11 | 5 | 86.5 | 89.5 |
| 51 | 3 | 4.5 | 22 | 11 | 5 | 93.6 | 98.8 |
| 52 | 3 | 2.5 | 18 | 8 | 13 | 85.4 | 84.7 |
| 53 | 3 | 3.5 | 28 | 11 | 5 | 93.5 | 98.5 |
| 54 | 3 | 4.5 | 22 | 8 | 13 | 97 | 92.8 |